Journal of New Materials for Electrochemical Systems 15, 271-276 (2012)

Synthesis and Characterization of RuO_2 Anode Materials with Large Surface Areas for Oxygen Evolution Reaction

Yang Zhang, Lixia Yue, Ke Teng, Shiyong Yuan and Hongchao Ma*

School of Chemistry Engineering & Material, Dalian Polytechnic University,
Dalian 116034, Liaoning China

Received: September 26, 2011, Accepted: January 10, 2012, Available online: February 17, 2012

Abstract: *A novel olivary or petal-like RuO_2 material with large surface area was successfully synthesized by surfactant-assisted homogeneous precipitation method using urea and dodecyl sulfate as the source reagent. The surface morphology, structural, and electrochemical properties of as-synthesized RuO_2 materials were characterized by x-ray diffraction (XRD), field-emission scanning electron microscopy (FE-SEM), Cyclic voltammetry (CV), N_2 adsorption–desorption isotherms and polarization curve for oxygen evolution reaction (OER). It was found that the morphology and crystalline structures and electrochemical properties of as-synthesized RuO_2 materials were strongly dependent on the calcining temperature. The ruthenium-surfactant mesophase with mesoporous structure transformed from network to regular olivary or petal-like RuO_2 materials and remaining partial mesoporous character after calcination at lower temperature (i.e., 300 and 400 °C). However, the mesophase transformed into RuO_2 agglomeration consisted of nanosized particles after calcination at 650 °C, which may be attributed to complete deorganization and porous structure collapse of RuO_2 materials. In addition, the as-synthesized RuO_2 materials showed higher specific surface area and better electrochemical activities for oxygen evolution reaction compared with the RuO_2 prepared without surfactant. The electrochemical activity of as-synthesized RuO_2 material calcined at 400 °C is about 3 times than that of RuO_2 prepared without surfactant for oxygen evolution reaction. This can be attributed to the porous structure and large surface area of as-synthesized RuO_2 materials.*

Keywords: RuO_2, high electrochemical activity, oxygen evolution, porous material, large surface area

1. INTRODUCTION

RuO_2 belongs to the family of transition-metal dioxide compounds with a rutile structure. It shows a high ohmic conductivity, as well as a high chemical and thermal stability. At present, RuO_2 materials has attracted a considerable attention because of its extensively applications for the industrial uses of chlorine generating anodes in the chlorine-alkali process, oxygen generating anodes in the electrolytic plating and as durable electrode in electrochemical and microelectronic devices[1-8]. Furthermore, RuO_2 is also used as a catalyst in the oxidation of CO[9], the combustion of ethylene[10], as well as pH electrodes[11] and supercapacitor system[12,13].

It is well known that the activity of RuO_2 has been attributed to both electronic and geometric effects. The former is attributed to the capacity of transition metals to exist in several valency states so that electron exchange with the environment is possible at several different redox potential levels. The latter is related to the high surface area as a consequence of the procedure of preparation of oxide materials. Although many synthetic procedure of RuO_2 materials have been developed, such as thermal decomposition of $RuCl_3$ in an organic medium [14], metal-organic chemical vapor deposition (MOCVD) [15], spin coating [16] and homogeneous preparation method using urea [17]. However, RuO_2 materials prepared by above synthetic routes is still unfavorable for its applications as electrodes because low specific surface area. As a attempt to synthesis of RuO_2 materials with high surface area, Oh et al reported a liquid crystal templating and crystallization route to synthesize mesoporous hydrous crystalline RuO_2 that exhibits high surface area (up to 250 m^2/g), a high capacitance of 410 F/g and good rate capability[18]. Thus, how to apparently enhance surface area of RuO_2 materials is an interesting topic because large surface area is often highly desirable for its applications as electrodes. In this work, a regular olivary or petal-like RuO_2 sheet with large

*To whom correspondence should be addressed: Email: m-h-c@sohu.com
Phone: (+86)-411-86323508 , Fax: (+86)-411-86323736

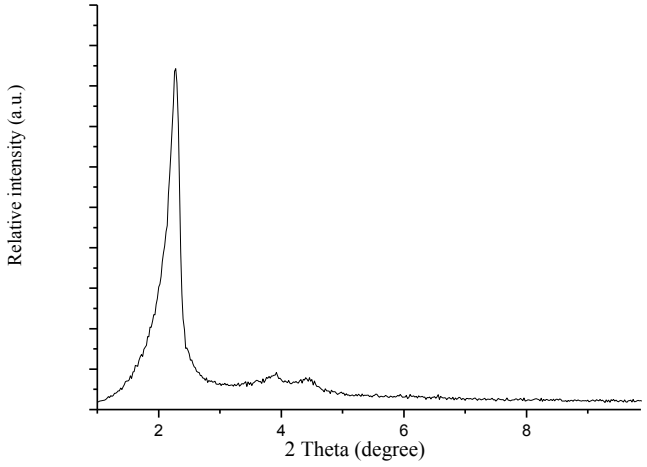

Figure 1. XRD pattern of the ruthenium-based dodecyl sulfate mesophase

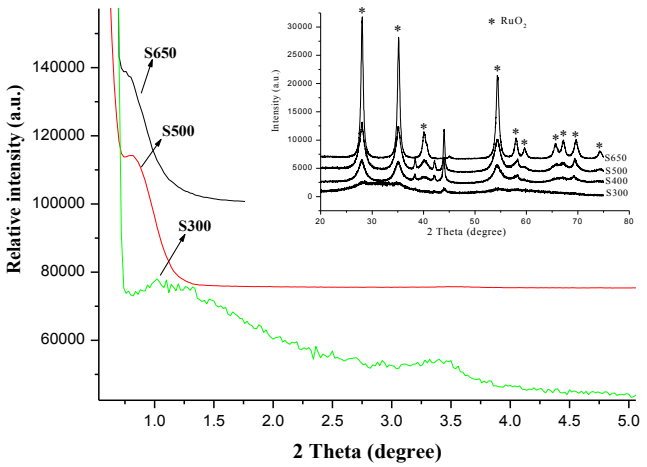

Figure 2. XRD patterns of the ruthenium-based dodecyl sulfate mesophase after calcinations

surface area was successfully synthesized by surfactant-assisted homogeneous precipitation method. The specific surface area of as-synthesized RuO_2 materials was up to 400 m^2/g, and was higher than that of RuO_2 materials in previous researches. Besides, the morphologies, textural characteristics and OER activities of the samples were also investigated.

2. EXPERIMENTAL

A fresh hydrated $RuCl_3$ (Ru assay=37.2%) by SPM Co. Ltd was used. Urea, sodium dodecyl sulfate (sds) and 30% H_2O_2 solution of analytical purity were supplied by Beijing chemical industry plant. Doubly distilled water was also used.

2.1. Samples preparation

Hydrated $RuCl_3$ was used as the ruthenium source and sodium dodecyl sulfate (sds, $CH_3(CH_2)_{12}OSO_3Na$) was used as the templating agent. In a typical procedure, $RuCl_3 \cdot nH_2O$, sds, urea and H_2O were mixed in a molar ratio of 1:2:40:600 and stirred at room temperature for 2h. This solution was heated up to 80 °C and then kept at this temperature until pH increased to 8 by hydrolysis urea for 6 h. The resulting mixture was immediately cooled to room temperature. After filtering and washing with doubly distilled water, a snuffcolored powder was obtained. The surfactant molecules were removed as follows: the ruthenium-based dodecyl sulfate mesophase was calcined at 300, 400, 500 and 650 °C for 5 h to remove their organic moieties with a heating rate of 10 °C min^{-1} in air which labeled them as S300, S400, S500 and S650, respectively.

For comparison, the RuO_2 catalyst was also synthesized by conventional homogeneous precipitation (i.e., there is lack of sds in above procedure). When pH of solution increased to 8, the precipitate was centrifuged, washed with doubly distilled water, dried at 80 °C overnight, and calcined under air at 400 °C for 5 h , to obtained resultant N400.

2.2. Samples characterization

X-ray powder diffraction measurements were performed at room temperature using a D/max 2500V PC X-ray diffractometer (Rigaku), with monochromatized CuK_α radiation. Morphology and particle sizes were analyzed in a XL30 ESEM FEG (FEI Co.) field-emission scanning electron microscope (FE-SEM).

Nitrogen physical adsorption–desorption isotherms were performed with a mictomeritics Asap model 2010 at 77 K, which were used to estimate specific surface area from BET[19].

Cyclic voltammetry (CV) studies were performed in a three-electrode configuration using a platinum plate counterelectrode and a saturated silver-chloride reference electrode. The working electrode was prepared by mixing the active material with 5wt% Nafion ionomer in ethanol solvent, which was made into slurry. A small drop of the slurry was added on to the mirror polished glassy-carbon substrate. The electrolyte was 1 M H_2SO_4 and the scan rate was 20 mV/s with the voltage range from 0 to 1.2 V referred to the saturated silver-chloride electrode. The voltammetric charges (q*) corresponding to active surface areas was determined by integrating the area of the cyclic curve.

The linear voltammetry measurements were carried out at 1 mV/s scan rate. The ohmic resistance between electrode surface and the capillary tip was very small, so it did not have any significant effect on the measured values in the potential range from 1.0 to 1.5 V. Hence, no IR compensation was used in these experiments. All electrochemical measurements were carried out at room temperature.

3. RESULTS AND DISCUSSION

The XRD pattern of precursor synthesized by surfactant-assisted homogeneous precipitation method only indicated three diffraction peaks at 2θ=1–5° shown in Fig.1. The three diffraction peaks can be assigned to the 100, 110 and 200 reflections based on hexagonal unit cell. The similar hexagonal structures have been observed for aluminium (or gallium)-based dodecyl sulfate [20, 21] and MCM-41 silica-surfactant composite materials [22]. Thus, the ruthenium-surfactant mesophase with mesostructure was obtained by surfactant-assisted homogeneous precipitation method.

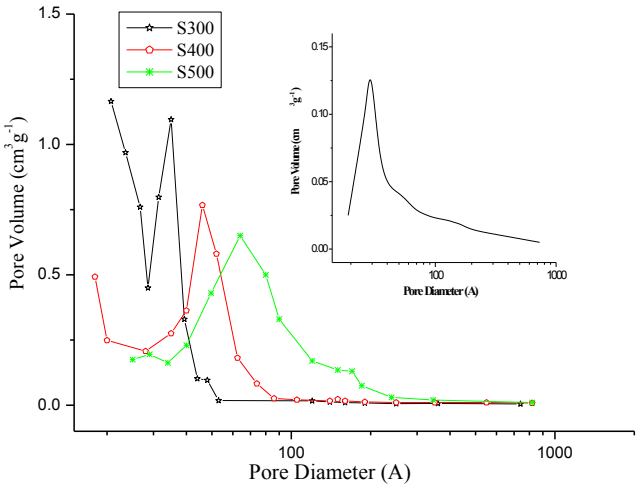

Figure 3. Pore-size distribution plots of samples

Low-angle XRD patterns of ruthenium-surfactant mesophase calcined at 300-650°C are shown in Fig.2. The XRD patterns of ruthenium-surfactant mesophase calcined at 300-650°C are differed from which was uncalcined. The sample S300 showed two discernible peaks at 2θ=1.26° and 2θ=3.4° corresponding to a expanded d-spacing of 69 and 26 Å, respectively. As calcining temperature increased, only one diffraction peak was found in X-ray diffraction patterns and shifted to lower angle, even this peak become indistinct after calcination at 500 °C. However, the XRD patterns indicated that the degree of ordering of the pore array was decreasing and the pore structure was gradually collapsed with the increasing of calcining temperature. Similar phenomenon was also reported by P. Salas et al in study on the sulfated Si–Zr–MCM-41 solid with highly ordered mesostructure [23].

Fig.2 insets is wide-angle XRD patterns of ruthenium-surfactant mesophase at 300-650°C. While increasing the temperature above 300°C, the XRD patterns of the materials can be indexed as tetragonal rutile structures RuO_2 according to JCPDS card (No.21-1172). The diffraction peak of RuO_2 become narrow with enhancing of temperature, which suggests that calcining temperature significantly alter the crystalline size. Meanwhile, three diffraction peaks of unkown-phase at 2θ values of 38.4°, 42.1° and 43.9° were also found in the XRD patterns of samples except for being calcined at 650°C, which imply that the deorganization of ruthenium-surfactant mesophases is incomplete when calcining temperature is lower than 650°C.

The pore size distribution of the samples is given in Fig.3. It can be seen that the most probable distribution of pore-size for ruthenium-surfactant precursor is about 29 Å (see Fig.3 insets), and the most probable distribution of pore-size for S300, S400 and S500 is about 35, 46 and 64 Å, respectively. Moreover, the most probable distribution of pore-size is gradually go broad with increasing of calcining temperature, which may be attributed to gradual collapse of ordered pore structure. The maximum of the pore-size distribution of samples shifts toward the high values of pore size as increasing of calcining temperature, which is in accordance with the expanded d-spacing of samples observed from in XRD patterns discussed previously.

In order to investigate the morphological change of precursor in calcining process, FE-SEM observations were carried out, and the results are shown in Fig.4. FE-SEM images of the ruthenium-based dodecyl sulfate mesophase are shown in Fig.4A. The ruthenium-based dodecyl sulfate mesophase shows an interesting network structure which consists of strips with a width of several micron. At the same time, the magnified image shows strips having a dissected tube-like shape. The formation of network morphology for ruthenium-based surfactant mesophase can be attributed to a similar growth and templating mechanism pathway of aluminium-based surfactant mesophases[24]. FE-SEM images of S300, S400 and S650 samples were shown in Fig.4B, C and D, respectively. It is observed that the morphology of the obtained mesophase changes from network-like to regular olivary or petal-like sheet after calcination at low temperature (300 and 400°C). However, the ruthenium-surfactant mesophase was deorganized into RuO_2 agglomeration consisted of nanosized particles after calcination at 650°C, which is attributed to complete removal of surfactant in mesophase. Whereas, the morphology of sample N400 (Fig.4E) prepared by normal method is markedly differs from above samples, its shape is very irregular, even larger crystal particle can be observed directly from the FE-SEM images.

Cyclic voltammograms of samples as OER electrode are shown in Fig.5. The irreversible peaks occurring around +0.5 V *vs* Ag/AgCl are attributed to the valence state change of the metal oxide from 3+ to 4+ in the RuO_2 [25]. Integration of the *j-E* curve provides the voltammetric charge, q*, which is proportional to the number of surface active sites. Thus, q* can be taken as a measure of the electrochemical surface area[26,27]. Fig.6 shows the calcining temperature dependence of the voltammetric charge q* and BET specific surface area of obtained RuO_2 materials. The S400 sample exhibited the maximum value of voltammetric charge q*. The calcining temperature dependence of the voltammetric charge q* differs from sequence of specific surface area calculated from BET method. As seen from Fig.6, the BET specific surface area of samples gradually decreased with increasing of calcining temperature, which was attributed to the collapse of porous structures. Moreover, the partial surface of porous RuO_2 material was still covered with surfactant after heat treatment at lower temperature, which decreases the amount of accessible electrochemical active sites. Apparently, 400°C is an appropriate calcining temperature for heat treatment of ruthenium-surfactant material used as porous electrode.

The Polarization curves of samples for OER are shown in Fig.7. The S400 sample showed the most OER activity at whole potentials. The OER activity sequence of samples is in good agreement with their electrochemical active area: S400>S500>S650>S300. This suggests that the activity of porous RuO_2 electrodes for OER rest with the extent of electrolyte-electrode interaction (electrochemical active area). The cyclic voltammograms of S400 and N400 samples are shown in Fig.8 inset. The voltammetric charge q* of S400 prepared by surfactant-assisted homogeneous precipitation is far larger than that of N400 prepared by conventional homogeneous precipitation, which suggests that the electrochemical active area of S400 is higher than that of N400. This can be attributed to that S400 have a larger surface area (the BET surface area of S400 and N400 are 404 and 89 m^2/g, respectively). As

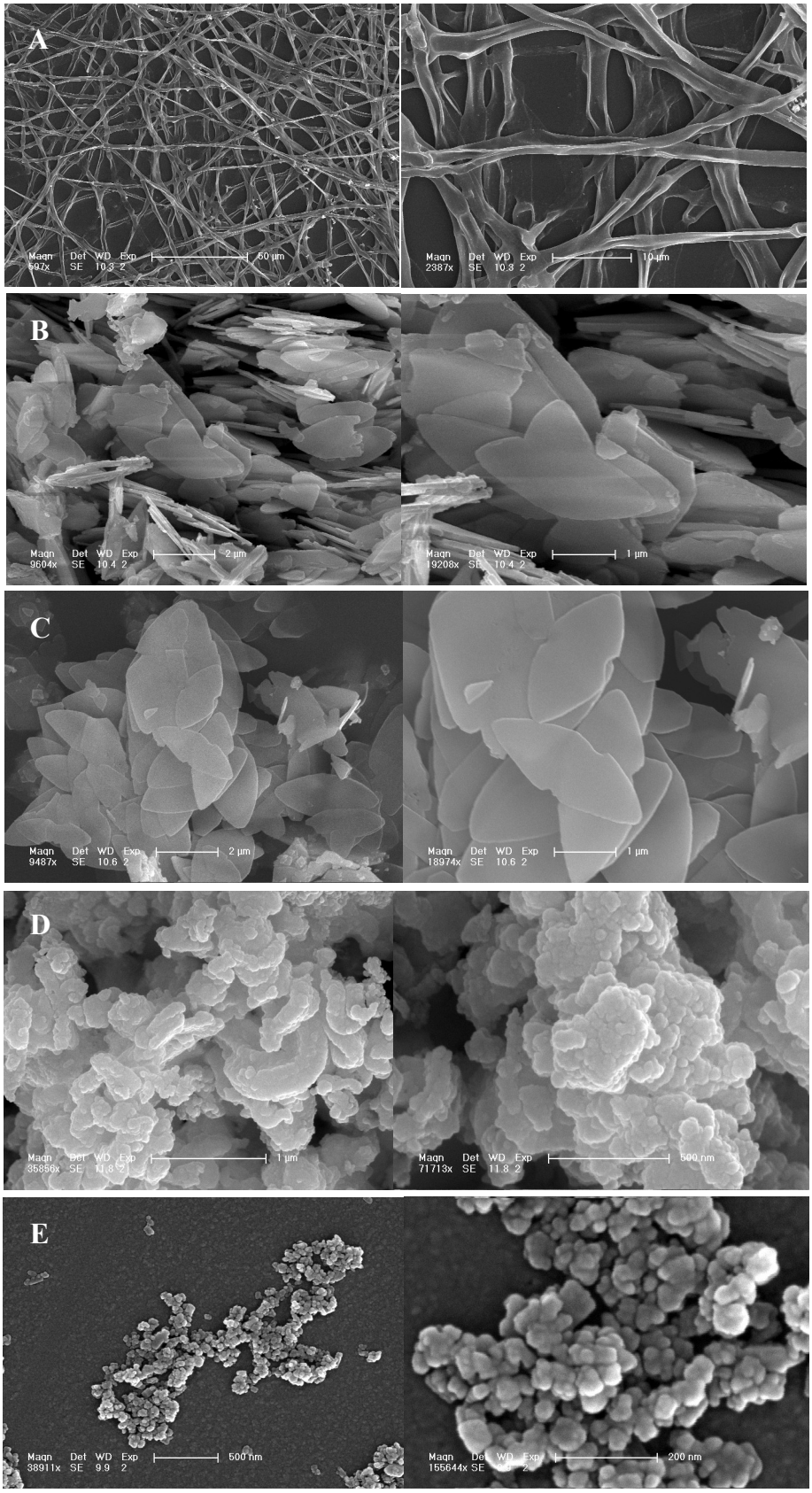

Figure 4. FE-SEM images of samples with low and high magnifications A . Ruthenium-based dodecyl sulfate precursor, B. S300, C. S400, D. S650, E. N400

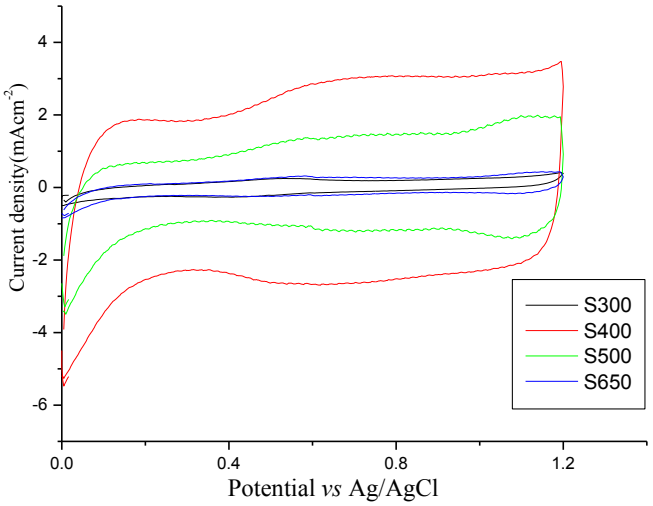

Figure 5. Cyclic voltammograms of samples in 1 M H_2SO_4

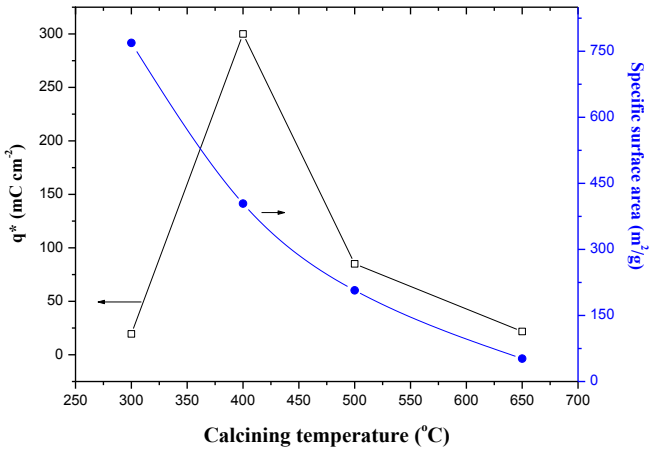

Figure 6. Dependence of voltammetric charge and specific surface areas of samples on calcining temperature.

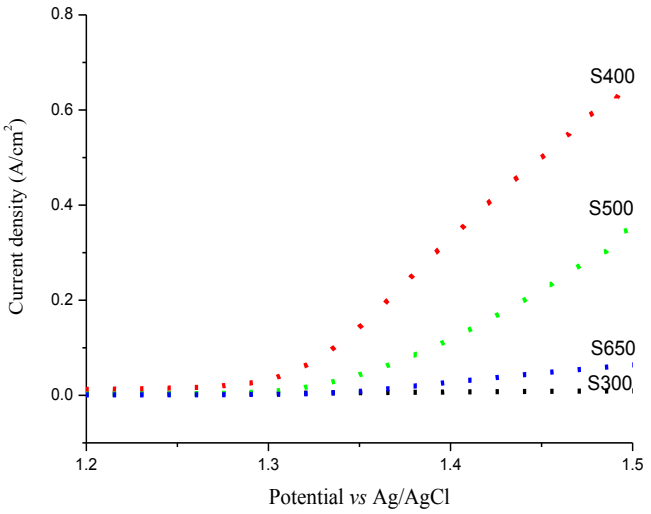

Figure 7. Polarization curve of samples for OER

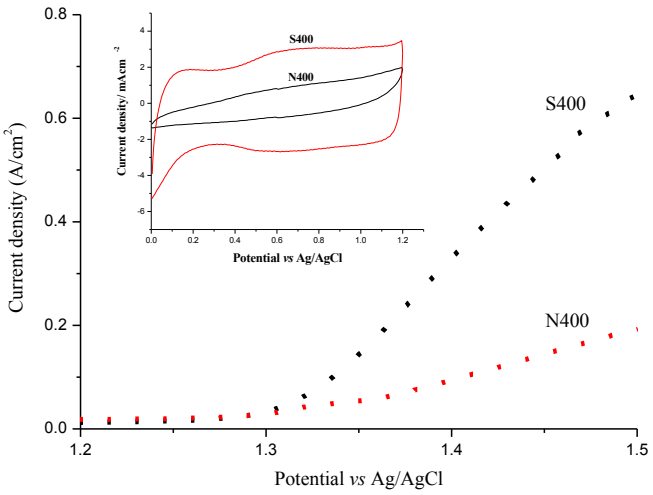

Figure 8. Polarization curve of S400 and N400 samples for OER

seen from Fig.8, the OER activity of S400 is far higher than that of N400, which is in good agreement with their electrochemical active area. Furthermore, the porous electrodes obtained by surfactant-assisted homogeneous precipitation method exhibited better OER activity as compared with the results reported in some literatures [28-30].

4. CONCLUSIONS

The RuO_2 material with large surface area can be obtained by surfactant-assisted homogeneous precipitation method, and showed higher activity for OER compared with RuO_2 material prepared without surfactant. It is found that the activity of porous RuO_2 electrodes for OER rest with the extent of electrolyte-electrode interaction (electrochemical active area). Moreover, enhancing specific surface area of RuO_2 material is one of efficient pathway to obtain RuO_2 material with high electrochemical active area. The electrochemical active area of RuO_2 material was strongly dependent on the calcining temperature. In this work, RuO_2 material calcined at 400℃ exhibited better OER activity. The resulting RuO_2 materials are expected to be useful as OER electrode.

5. ACKNOWLEDGEMENTS

This work was supported by Program for Liaoning Excellent Talents in University (LGQ-2011-054).

REFERENCES

[1] M.T. Brumbach, T.M. Alam, P.G. Kotula, ACS Appl. Mat. Interfaces, 2, 778 (2010).
[2] A.S. Kumar, T.Tanase, J. Zen, Langmuir, 25, 13633 (2009).
[3] K.C. Pillai, T.O. Kwon, B.B. Park, Water Sci.Tech., 61, 2151 (2010).
[4] S.Trasatti, G. Buzzanca, J. Electroanal. Chem., 29, 1 (1971).
[5] J. Lee, H. Chen, H.M. Wu, T. Wei, Electrochim. Acta, 52, 2625 (2007).

[6] K.M. Sujit, N. Munichandraiah, J. Power Sources, 175, 657 (2008).
[7] T.P. Gujar, V.R. Shinde, C.D. Lokhande, Electrochem. Comm., 9, 504 (2007).
[8] W.P. Gan, Z.H. Qin, H. Liu, Materials Review, 22, 143 (2008).
[9] L. Zang, H. Kisch, Angew. Chem, Int. Ed., 39, 3921 (2000).
[10]S. Wodiunig, V. Patsis, C. Comninellis, Solid State Ion., 136-137, 813 (2000).
[11]R. Koncki, M. Mascini, Anal.Chim. Acta, 351, 143 (1997).
[12]B.E. Conway, J. Electrochem. Soc., 138, 1539 (1991).
[13]J.P. Zheng, P.J. Cygan, T.R. Jow, J. Electrochem. Soc., 142, 2699 (1995).
[14]Yasushi Murakami, Takeshi Kondo, Yoshio Takasu, J. Alloys and Compounds, 239, 111 (1996).
[15]S.Y. Mar, Y.S. Huang and K.K. Tiong, *Thin Solid Films*, 258, 104 (1995).
[16]J.H. Yi, P. Thomas, M. Manier, J.P. Mercurio, J. Phys., IV Fr., 8, 9 (1998).
[17]F. Porta, W.P. Hsu, E. Matijević, Colliods Surf., 46, 63 (1990).
[18]S.H. Oh, L.F. Nazar, J. Mater. Chem., 20, 3834 (2010).
[19]S. Brunauer, P.H. Emmet, E. Teller, J. Am. Chem. Soc., 60, 309 (1938).
[20]Mitsunori Yada, Masato Machida, Tsuyoshi Kijima, Chem. Commun., 769 (1996).
[21]Mitsunori Yada, Hiroyuki Takenaka, Masato Machida, Tsuyoshi Kijima, J.Chem. Soc. Dalton Trans., 1547 (1998).
[22]C.T. Kresge, M.E. Leonowicz, J.C. Vartuli, J.S. Beck, Nature, 359, 710 (1992).
[23]P. Salas, L.F. Chen, J.A. Wang, H. Armendáriz, M.L. Guzman, J.A. Montoya, D.R. Acosta, Applied Surface Science, 252, 1123 (2005).
[24]P.D. Yang, D.Y. Zhao, D.I. Margolese, B.F. Chmelka, G.D. Stucky, Nature, 396, 152 (1998).
[25]K. Dobelhofer, M. Metikos, Z. Ogumi, H. Gerischer, Ber, Bunsenges. Phys. Chem., 82, 1046 (1978).
[26]B. Aurian-Blajeni, A.G. Kimball, L.S. Robblee, G.L.M.K.S. Kahanda, M. Tomkiewicz, J. Electrochem. Soc., 134, 2637 (1987).
[27]R. Boggio, A. Carugati, S. Trasatti, J. Applied Electrochem., 828, 17 (1987).
[28]L.J. Zhao, Z.X. Liu, P. Zhang, Z.Q. Mao., Batt Bimonth., 40, 19 (2010).
[29]Etsushi Tsuji, Akihito Imanishia, Ken-ichi Fukui, Yoshihiro Nakato, Electrochim. Acta, 56, 2009 (2011).
[30]W. Xu, Jyoti Tayal, Suddhasatwa Basu, Keith Scott., Int. J. Hydrogen Energy, 36, 14796 (2011).